Comput Geosci (2007) 11:131–144
DOI 10.1007/s10596-007-9045-y

ORIGINAL PAPER

A coupling of mixed and continuous Galerkin finite element methods for poroelasticity I: the continuous in time case

Phillip Joseph Phillips · Mary F. Wheeler

Received: 24 May 2005 / Accepted: 1 December 2006 / Published online: 22 March 2007

Abstract In this paper, we formulate a finite element procedure for approximating the coupled fluid and mechanics in Biot's consolidation model of poroelasticity. Here, we approximate the pressure by a mixed finite element method and the displacements by a Galerkin method. Theoretical convergence error estimates are derived in a continuous in-time setting for a strictly positive constrained specific storage coefficient. Of particular interest is the case when the lowest-order Raviart–Thomas approximating space or cell-centered finite differences are used in the mixed formulation, and continuous piecewise linear approximations are used for displacements. This approach appears to be the one most frequently applied to existing reservoir engineering simulators.

P. J. Phillips
Center for Subsurface Modeling (CSM),
Institute for Computational Engineering and Sciences
(ICES), University of Texas at Austin, Austin, TX, USA

M. F. Wheeler (✉)
CSM, ICES, Department of Aerospace Engineering
and Engineering Mechanics, University of Texas at Austin,
Austin, TX, USA
e-mail: mfw@ices.utexas.edu

M. F. Wheeler
Department of Petroleum Engineering and Geosystems
Engineering, University of Texas at Austin,
Austin, TX, USA

M. F. Wheeler
Institute for Computational Engineering and Sciences,
University of Texas at Austin, Austin, TX, USA

Keywords Continuous Galerkin · Continuous in time a priori error estimates · Mixed finite elements · Poroelasticity

1 Introduction

Poroelasticity[1] – the modeling of coupled mechanics and flow in porous media – is of increasing importance today in a diverse range of engineering fields. Notable contributions of poroelasticity have been made to areas that include reservoir engineering, biomechanics, and environmental engineering, and promising possibilities hold for fields like earthquake engineering.

In reservoir engineering, terms like *consolidation*, the reduction in volume of a porous medium due to fluid extraction; *compaction*, volume reduction due to air removal; and *subsidence*, vertically oriented consolidation or compaction, have entered the nomenclature as a result of the observed side effects of drilling. Sometimes, the effects of fluid flow-induced deformations are harmless, but there are indeed vivid examples that remind that the fluid–solid coupling cannot be ignored. In [18], Dean discusses one such case of an oil company's platforms in the North Sea at Ekofisk field:

> They subsided so much they had to go in and raise the platforms, costing them several billion dollars. If they'd known ahead of time, they could have built their platforms taller.

"Knowing ahead of time" is precisely why poroelastic modeling has come to be viewed as an important tool

[1] A term coined by J. Geertsma in 1966 [33].

by which reservoir engineers might attempt to avert future financial calamities. Predicting drilling-induced subsidence can sometimes be accomplished by running computer simulations of various injection/extraction well configurations. Another frequent problem confronting the petroleum industry is borehole damage caused by the shifting subsurface. Related work can be found (see [7, 10, 23]); other work that also includes thermal effects is found in [34].

In biomechanics, Roose et al. [26] used a poroelastic model to estimate tumor-induced stress levels in the brain, and thereby assist in a clinical diagnostic setting; Smillie et al. [29] likewise modeled the brain, but in this case, their goal was to study the pathological condition hydrocephalus, which induces an irregular cerebrospinal fluid flow, thus causing the brain to undergo potentially lethal deformations. Others, like Swan et al. [30], used poroelastic modeling of bone in order to estimate optimal (external) mechanical loading in order to produce effective bone adaptation. Still others used poroelasticity to assist in their development of prosthetic devices (for cartilage, bone, heart valves, etc.).

In environmental engineering, researchers are often concerned with understanding and, if necessary, limiting the unintended effects from such activities as groundwater pumping or oil extraction on the environment. One well-known case is where excessive groundwater removal caused Venice to start sinking [18]. Langford [14] pointed to the same problem in Houston, TX, and how city planners are attempting to avoid further subsidence by converting primarily to surface water usage. Another environmentally related problem is the attempt to control seepage flow from buried hazardous waste sites to local groundwater. The poroelastic model of [13] can be applied to this problem; the nuclear waste disposal problem is similarly tackled in [12] and [27].

Within the field of earthquake engineering, a term from poroelasticity that is frequently used is *liquefaction* – the state in which the fluid pressure in a porous medium becomes greater than the forces holding the solid together, and thus converting the mostly solid-like structure to a more fluid-like structure. Tectonic shaking induces an increase in subsurface fluid pressure and thus potentially devastating liquefaction. One such example was the 1964 Niigata earthquake when liquefaction caused many apartment buildings to be overturned. As the Civil Engineering Department at the University of Washington points out on their website, there are basically three ways to mitigate liquefaction hazards: (1) avoid liquefaction-susceptible soils, (2) build liquefaction-resistant structures, and (3) improve the soil. The latter two methods can benefit from the use of poroelastic model-based computer simulations. In [16], one of the most highly cited experts in earthquake engineering, Dr. Jian Lin pointed to poroelastic modeling as one of the reasons that he saw "... an exciting possibility that future models will have significantly improved predictive capability."

Because of the complicated nature of the equations, only a few nontrivial analytical series solutions have been found. The problems of Terzaghi (one-dimensional), Mandel (two-dimensional), and Barry and Mercer (two-dimensional) are examples of problems with such solutions. Conversely, whereas analytical solutions have been rare, there have been numerous numerical solutions to various problems. Although some groups have used finite difference methods, such as the aforementioned one led by Roose, most have used finite element methods and utilized continuous Galerkin elements for both the displacements and pressure. Lewis and Schrefler [15] presented and applied such methods to one- and two-dimensional problems in consolidation and to the problem of subsidence in Venice. Other numerical work has been conducted at the Center for Subsurface Modeling, at the University of Texas at Austin. There, Liu [17] implemented a scheme involving Taylor–Hood elements and, subsequently, a DG variant based on the work of Phillips and Wheeler. He also implemented a model that includes thermal effects and a plasticity model for the porous medium. Also at the Center for Subsurface Modeling, Gai [9] used continuous elements for displacements and a cell-centered finite difference (CCFD) method for pressure, but implemented an iteratively coupled scheme to find the numerical solution. She also tackled the multiphase flow version of the poroelasticity equations.

With the progress that has been made in the computational realm, there has also been concurrent increase in the attention given to a priori error estimates. In 1996, Murad, Thomee, and Loula provided the first error estimates, but in a restricted sense. They assumed a null constrained specific storage coefficient value, $c_o = 0$, and they considered only the case of zero Dirichlet conditions for both pressure and displacements and an initial condition of $\nabla \cdot \mathbf{u}(0) = 0$. These are somewhat unnatural conditions and create a problem because in the limit $t \to 0$, the poroelasticity problem reduces to Stokes problem with homogenous Dirichlet pressure boundary conditions. Wheeler and Phillips [37] later proposed an algorithm that models displacements with continuous elements and the flow with a mixed method. They then described their results of optimal continuous-in-time and discrete-in-time error estimates

for general boundary and initial conditions for the case $c_o > 0$. It is then the purpose of this paper and its sequel to supply the proofs of our findings.

The rest of this paper is organized as follows: Section 2 describes the Biot's consolidation model. In Section 3, we formulate the numerical method and establish existence and uniqueness. In Section 4, we state and prove continuous convergence results. Lastly, Section 5 presents some of our numerical results.

2 Model formulation

2.1 Derivation of the model

The poroelasticity equations consist of a momentum and a mass conservation equation and are derived at the macroscopic scale in the work of Terzaghi [31] and Biot [2, 3]. In our discussion of the equations, we follow the presentation of Showalter [28].

The momentum conservation is similar to that found in linear elasticity, the exception being the addition of a fluid pressure term. Because the deformation of the material is usually much slower than the flow rate, a quasistatic assumption is made, so that the second time derivative for displacements is ignored. To derive the momentum equation, let $\Omega \subset R^d$, and choose V to be a fixed, arbitrary open subset of Ω. Then, for the total stress tensor, $\tilde{\boldsymbol{\sigma}}$, and a body force, $\mathbf{f}$, we have

$$-\int_{\partial V} \tilde{\boldsymbol{\sigma}}\boldsymbol{\nu}\,\mathrm{d}s = \int_V \mathbf{f}\,\mathrm{d}V,$$

where $\boldsymbol{\nu}$ is the outward normal. Using the divergence theorem on the left side allows us to conclude:

$$-\int_V \nabla\cdot\tilde{\boldsymbol{\sigma}}\,\mathrm{d}V = \int_V \mathbf{f}\,\mathrm{d}V.$$

Because V was chosen arbitrarily, it follows that $-\nabla\cdot\tilde{\boldsymbol{\sigma}} = \mathbf{f}$ over Ω.

Turning to the mass conservation equation, we again let $V \subset \Omega$ be a fixed, arbitrary open subset of Ω. We refer to η as the fluid content of the medium, $\mathbf{v}_\mathrm{f}$ as its flux, and h as the volumetric fluid source term. We then conclude from elementary conservation principles

$$\frac{\partial}{\partial t}\int_V \eta\,\mathrm{d}V = -\int_{\partial V}\mathbf{v}_\mathrm{f}\cdot\boldsymbol{\nu}\,\mathrm{d}s + \int_V h\,\mathrm{d}V.$$

Then, using the divergence on the first term on the right side of the above equation and the fact that V was chosen arbitrarily implies that

$$\frac{\partial\eta}{\partial t} = -\nabla\cdot\mathbf{v}_\mathrm{f} + h.$$

In order to close the model, constitutive relations must be formulated to relate the total stress $\tilde{\boldsymbol{\sigma}}$, flux $\mathbf{v}_\mathrm{f}$, and fluid content η to the primary variables pressure p and deformation $\mathbf{u}$ (see Table 1). The total stress must account for the usual material stress as in elasticity and for the fluid pressure; consequently, we set $\tilde{\boldsymbol{\sigma}} = \boldsymbol{\sigma} - \alpha\nabla p$. Here, $\boldsymbol{\sigma}$ is the standard stress tensor from elasticity (which we assume to be a linear function of $\mathbf{u}$) and is referred to as the "effective stress" in the field of poroelasticity. The pressure term measures the effect of fluid of the material medium; an increase in pressure generally causes an expansion. The standard assumption of *Darcy's* law from porous media holds for the flux, and we set $\mathbf{v}_\mathrm{f} = -\frac{1}{\mu_\mathrm{f}}\boldsymbol{\kappa}(\nabla p - \rho_\mathrm{f}\mathbf{g})$. The permeability tensor $\boldsymbol{\kappa}$ is assumed to be uniformly bounded and uniformly elliptic; that is, there exist positive constants $\lambda_{\min}$ and $\lambda_{\max}$, such that for all $x \in \Omega$, the following relation holds:

$$\lambda_{\min}||\boldsymbol{\xi}||^2 \;\le\; \boldsymbol{\xi}^t\boldsymbol{\kappa}(\mathbf{x})\boldsymbol{\xi} \;\le\; \lambda_{\max}||\boldsymbol{\xi}||^2. \tag{2.1}$$

It is natural to assume that the amount of fluid content η depends on the fluid pressure p and the material volume, which is measured locally by $\nabla\cdot\mathbf{u}$. More specifically, we set $\eta = c_\mathrm{o}p + \alpha\nabla\cdot\mathbf{u}$ and observe that $c_\mathrm{o}p$ measures the amount of fluid that can be injected into a fixed material volume, and $\alpha\nabla\cdot\mathbf{u}$ measures the amount of fluid that can be squeezed out. The constrained specific storage coefficient c_o may, in general, be zero, but in this paper, it is assumed to be strictly positive:

$$c_\mathrm{o} \ge \gamma_\mathrm{o} > 0 \tag{2.2}$$

for some positive constant γ_o (see Table 2).

Table 1 Summary of constitutive relations

$\tilde{\sigma}_{ij}(\mathbf{u}, p)$	=	$\sigma_{ij}(\mathbf{u}) - \alpha\delta_{ij}p$	Total stress
$\sigma_{ij}(\mathbf{u})$	=	$\lambda\delta_{ij}\epsilon_{kk}(\mathbf{u}) + 2\mu\epsilon_{ij}(\mathbf{u})$	Effective stress
η	=	$c_\mathrm{o}p + \alpha\nabla\cdot\mathbf{u}$	Fluid content
$\mathbf{v}_\mathrm{f}$	=	$-\frac{1}{\mu_f}\boldsymbol{\kappa}(\nabla p - \rho_f\mathbf{g})$	Volumetric fluid flux

Table 2 Summary of physical parameters

Parameter	Description
λ, μ	Positive Lamé constants
c_o	Constrained Specific Storage Coefficient
α	Biot–Willis
$\boldsymbol{\kappa}$	Symmetric permeability tensor
μ_f	Fluid viscosity

The momentum and mass conservation equations are coupled through the *Biot–Willis* constant α, which is usually close to unity. The material parameters are usually found experimentally or through some homogenization technique.

2.2 Summary of the poroelasticity equations

We summarize the governing equations below and complete the model by including the necessary boundary and initial conditions. There are two distinct sets of boundary conditions, one corresponding to the flow and one corresponding to the deformation.

$$-(\lambda+\mu)\nabla(\nabla\cdot\mathbf{u})-\mu\nabla^2\mathbf{u}+\alpha\nabla p=\mathbf{f}, \tag{2.3a}$$

$$\frac{\partial}{\partial t}(c_{\mathrm{o}}p+\alpha\nabla\cdot\mathbf{u})-\frac{1}{\mu_{\mathrm{f}}}\nabla\cdot\boldsymbol{\kappa}(\nabla p-\rho_{\mathrm{f}}\mathbf{g})=h, \tag{2.3b}$$

$$p(t)=p_{\mathrm{o}} \quad \text{on} \quad \Gamma_{\mathrm{p}}, \tag{2.4a}$$

$$-\frac{1}{\mu_{\mathrm{f}}}\boldsymbol{\kappa}(\nabla p-\rho_{\mathrm{f}}\mathbf{g})\cdot\boldsymbol{\nu}=q \quad \text{on} \quad \Gamma_{\mathrm{f}}, \tag{2.4b}$$

$$\mathbf{u}(t)=\mathbf{u}_D \quad \text{on} \quad \Gamma_{\mathrm{o}}, \tag{2.4c}$$

$$\tilde{\boldsymbol{\sigma}}\boldsymbol{\nu}=\mathbf{t}_N \quad \text{on} \quad \Gamma_{\mathrm{t}}, \tag{2.4d}$$

$$p(0)=p^o, \tag{2.4e}$$

$$\mathbf{u}(0)=\mathbf{u}^o, \tag{2.4f}$$

where $\partial\Omega=\Gamma_{\mathrm{p}}\bigcup\Gamma_{\mathrm{f}}$ and $\partial\Omega=\Gamma_{\mathrm{t}}\bigcup\Gamma_{\mathrm{o}}$. Also, $\boldsymbol{\nu}$ represents the outward normal to $\partial\Omega$.

Remark 2.1 Often in practice, initial conditions are found by first setting $p(0)$ equal to the hydrostatic pressure (which amounts to solving $\nabla p(0)=\rho_f\mathbf{g}$), and then using $p(0)$ in Eq. 2.3a to solve for $\mathbf{u}(0)$.

The most complete work to date on the mathematical properties of solutions to Eqs. 2.3a and 2.3b is undertaken by Showalter [28]. The author's theoretical work assumed that the Dirichlet boundary terms for the pressure and displacement are null, and his Neumann boundary conditions differ somewhat from those considered here. His initial conditions also differ slightly and require a certain compatibility condition. With the further assumption that all the source data are functions in $C^{\beta}([0,T];L^2)$ (Hölder continuous), the existence and uniqueness of a pressure p and displacement $\mathbf{u}$ solution are proved. The regularity is shown to satisfy

$$||\mathbf{u}(t)||_3+||p(t)||_2\leq\frac{C}{t}. \tag{2.5}$$

Other work involving weak solutions has been undertaken by Zenisek [38] for the case that $c_{\mathrm{o}}=0$ and by Phillips [21] for the general case $c_{\mathrm{o}}\geq 0$.

3 The coupled formulation

This section presents a finite element algorithm for linear poroelasticity that couples continuous Galerkin elements for displacements with a mixed space formulation for flow (CG/Mixed). The primary motivations for doing so are threefold:

1. Flux a primary variable. This eliminates the need to use postprocessing techniques to produce the flux from the numerical pressure.
2. Element-wise mass conservation. By construction of the mixed space, the flux normal is continuous across element boundaries, thus ensuring local mass conservation.
3. Error estimates for CCFD. Many commercial flow simulators use a CCFD method to simulate flow. Because CCFD is equivalent to the mixed method with reduced integration [35], there is the potential to reuse the time-tested CCFD code in the linear poroelasticity algorithm presented here and maintain the optimality of the error estimates.

Our fully coupled algorithm includes a mixed formulation for flow, so we first introduce the variable for the flux, $\mathbf{z}=-\frac{1}{\mu_{\mathrm{f}}}\boldsymbol{\kappa}(\nabla p-\rho_{\mathrm{f}}\mathbf{g})$, and set $\tilde{\boldsymbol{\kappa}}=\frac{1}{\mu_f}\boldsymbol{\kappa}$. Equations 2.3a and 2.3b then become

$$-(\lambda+\mu)\nabla(\nabla\cdot\mathbf{u})-\mu\nabla^2\mathbf{u}+\alpha\nabla p=\mathbf{f}, \tag{3.1a}$$

$$\frac{\partial}{\partial t}(c_{\mathrm{o}}p+\alpha\nabla\cdot\mathbf{u})+\nabla\cdot\mathbf{z}=h, \tag{3.1b}$$

$$\tilde{\boldsymbol{\kappa}}^{-1}\mathbf{z}+\nabla p=\rho_{\mathrm{f}}\mathbf{g}. \tag{3.1c}$$

This set of equations will serve as the basis for a variational formulation. In order to proceed, we first define suitable function spaces.

3.1 Bilinear form and function spaces

For the mixed formulation developed herein, the appropriate function space for the pressure is $L^2(\Omega)$. The space used for the flux variable is $H(\mathrm{div})\equiv\{\mathbf{s}\in(L^2(\Omega))^d:\nabla\cdot\mathbf{s}\in L^2(\Omega)\}$. With $H(\mathrm{div})$, we then define the following subset:

$$\mathbf{S}_0\equiv\{\mathbf{s}\in H(\mathrm{div}):\mathbf{s}\cdot\boldsymbol{\nu}|_{\Gamma_{\mathrm{f}}}=0\}.$$

The function space relevant to the deformation is

$$\mathbf{V}_0\equiv\{\mathbf{v}\in(H^1(\Omega))^d:\mathbf{v}|_{\Gamma_{\mathrm{o}}}=0\}.$$

Associated to this space is the bilinear form defined as

$$a_{\mathbf{u}}(\mathbf{u},\mathbf{v}) \equiv \int_{\Omega} \boldsymbol{\sigma}(\mathbf{u}) : \epsilon(\mathbf{v}) \mathrm{d}x.$$

The linearized *strain* tensor is given by $\epsilon_{kl} \equiv \frac{1}{2}(\partial_k u_l + \partial_l u_k)$, and thus

$$a_{\mathbf{u}}(\mathbf{u},\mathbf{v}) = \int_{\Omega} (2\mu(\epsilon(\mathbf{u}) : \epsilon(\mathbf{v})) + \lambda(\nabla \cdot \mathbf{u})(\nabla \cdot \mathbf{v})) \mathrm{d}x. \tag{3.2}$$

Here, $(\sigma : \tau) = \sum_i \sum_j \sigma_{ij}\tau_{ij}$. Clearly, $a_{\mathbf{u}}(,)$ is symmetric and continuous. Furthermore, given that $|\Gamma_o| > 0$, *Korn's inequality* shows that $a_{\mathbf{u}}(,)$ is also coercive on $\mathbf{V}_0$ (see [5]). With the energy norm defined as $||\mathbf{u}||^2_{a_{\mathbf{u}}} \equiv a_{\mathbf{u}}(\mathbf{u},\mathbf{u})$, the following inequalities hold for some positive real numbers C_{cont} and C_{coer}:

$$a_{\mathbf{u}}(\mathbf{u},\mathbf{v}) \le C_{\mathrm{cont}} ||\mathbf{u}||_{H^1} ||\mathbf{v}||_{H^1}, \quad \forall \mathbf{u},\mathbf{v} \in H^1, \tag{3.3}$$

$$C_{\mathrm{coer}} ||\mathbf{u}||^2_{H^1} \le ||\mathbf{u}||^2_{a_{\mathbf{u}}}, \quad \forall \mathbf{u} \in \mathbf{V}_0. \tag{3.4}$$

We now provide some definitions important for the development of our finite element scheme. Our notation follows Rivière and Wheeler [25]. Let $\mathcal{E}_h = \{E_1, E_2, ..., E_{M_h}\}$ be a nondegenerate subdivision of Ω, where E_j is a triangle or a convex quadrilateral for $d = 2$, or a tetrahedron if $d = 3$. Let $h_j = \mathrm{diam}(E_j)$; then, nondegeneracy requires the existence of $\rho > 0$, such that E_j contains a ball of radius ρh_j. We also set $h = \max\{h_j : j = 1, ..., M_h\}$.

The finite dimensional approximating spaces are defined as follows: Let $(W_h, \mathbf{S}_h) \subset (L^2 \times H(\mathrm{div}))$ denote a standard mixed finite element space defined on $\mathcal{E}_h$; in particular, let $\mathbf{S}_{h,0} \equiv \{\mathbf{s} \in \mathbf{S}_h : \mathbf{s} \cdot \boldsymbol{\nu}|_{\Gamma_f} = 0\}$. Let k refer to the order of this space. Additionally, these spaces are required to be endowed with two linear operators, $\Pi_h : H(\mathrm{div}) \to \mathbf{S}_h$ and the L^2 projection $L^2 \to W_h$, which satisfy the following properties:

$$(\nabla \cdot (\mathbf{s} - \Pi_h \mathbf{s}), w) = 0, \quad \forall w \in W_h, \tag{3.5a}$$

$$||\mathbf{s} - \Pi_h \mathbf{s}||_{L^2} \le C h^r ||\mathbf{s}||_{H^r}, \quad 1 \le r \le k+1, \tag{3.5b}$$

$$\nabla \cdot \Pi_h = P_h \nabla \cdot, \tag{3.5c}$$

$$(\nabla \cdot \mathbf{s}_h, p - P_h p) = 0, \quad \forall \mathbf{s}_h \in \mathbf{S}_h, \tag{3.5d}$$

$$||p - P_h p||_{L^2} \le C h^r ||p||_{H^r}, \quad 0 \le r \le k+1. \tag{3.5e}$$

The Raviart–Thomas–Nedelec space of order $k = 0$ (see [20, 24]) is one example and is used for the numerical examples that follow. Note that not all mixed-spaces operators satisfy each of the above properties, in particular, Eq. 3.5b, where the upper bound for r is sometimes only k.

Regarding the deformation space, we let $\mathbf{V}_h$ be the space of continuous piecewise polynomials of degree r; set $\mathbf{V}_{h,0} \equiv \{\mathbf{v} \in \mathbf{V}_h : \mathbf{v}|_{\Gamma_o} = 0\}$. The elliptic projection operator $\tilde{P}$: $(H^1)^d \to \mathbf{V}_h$ (see [36]) will be used in the following theorem; $\tilde{P}$ satisfies

$$a_{\mathbf{u}}(\mathbf{u} - \tilde{P}\mathbf{u}, \mathbf{v}_h) = 0 \quad \forall \mathbf{v}_h \in \mathbf{V}_h.$$

The following inequality describes its approximation properties:

$$||\mathbf{u} - \tilde{P}\mathbf{u}||_{a_{\mathbf{u}}} \le C h^{s-1}, \quad 1 \le s \le r+1. \tag{3.6}$$

3.2 Coupled algorithm

In order for the variational formulation presented below to make sense, the following regularity requirements on the data are assumed:

$$\mathbf{f} \in C^1([0,T]; (H^{-1}(\Omega))^d), \tag{3.7}$$

$$h \in C^0([0,T]; L^2(\Omega)), \tag{3.8}$$

$$p_o \in C^0([0,T]; L^2(\Gamma_p)), \tag{3.9}$$

$$q \in C^0([0,T]; TrS), \tag{3.10}$$

$$\mathbf{u}_D \in C^1([0,T]; (H^{1/2}(\Gamma_o))^d), \tag{3.11}$$

$$\mathbf{t}_N \in C^1([0,T]; (H^{-1/2}(\Gamma_t))^d). \tag{3.12}$$

Here, $TrS \equiv \{\mathbf{s} \cdot \boldsymbol{\nu}|_{\Gamma_f} : \mathbf{s} \in H(\mathrm{div})\}$. As for the initial time data, we require that $\mathbf{u}^o \in (H^1)^d$ and $p^o \in L^2$.

In order to produce a variational formulation, we multiply Eq. 3.1a by $\mathbf{v} \in \mathbf{V}_0$ and Eqs. 3.1b and 3.1c by $(w, \mathbf{s}) \in L^2 \times \mathbf{S}_0$. The formulation is completed by integrating each of the equations over Ω and integrating by parts when necessary. Now, the essential boundary conditions for the displacement and flux are allowed to be inhomogeneous, so it is necessary to work in affine spaces. So, for each $t \ge 0$, select some $\mathbf{u}_d(t,\mathbf{x}) \in (H^1)^d$ such that $\mathbf{u}_d(t,\mathbf{x})|_{\Gamma_o} = \mathbf{u}_D(t,\mathbf{x})$, and choose some $\mathbf{z}_d(t,\mathbf{x}) \in H(\mathrm{div})$ such that $\mathbf{z}_d(t,\mathbf{x}) \cdot \boldsymbol{\nu}|_{\Gamma_f} = q(t,\mathbf{x})$. With this, the variational problem becomes: find $\mathbf{u} \in \mathbf{u}_d + H^1([0,T]; \mathbf{V}_0)$, $p \in H^1([0,T]; L^2)$ and $\mathbf{z} \in \mathbf{z}_d + L^2([0,T]; \mathbf{S}_0)$, such that

$$a_{\mathbf{u}}(\mathbf{u},\mathbf{v}) - \alpha(\nabla \cdot \mathbf{v}, p) = l_1(\mathbf{v}), \tag{3.13}$$

$$(c_o p_t, w) + \alpha(\nabla \cdot \mathbf{u}_t, w) + (\nabla \cdot \mathbf{z}, w) = l_2(w), \tag{3.14}$$

$$(\tilde{\boldsymbol{\kappa}}^{-1}\mathbf{z}, \mathbf{s}) - (p, \nabla \cdot \mathbf{s}) = l_3(\mathbf{s}). \tag{3.15}$$

holds for every $t \in [0, T]$ and $(\mathbf{v}, w, \mathbf{s}) \in (\mathbf{V}_0, L^2, \mathbf{S}_0)$. Here, l_1, l_2, and l_3 are bounded linear functionals defined as

$$l_1(\mathbf{v}) = \int_\Omega \mathbf{f} \cdot \mathbf{v} + \int_{\Gamma_t} \mathbf{t}_N \cdot \mathbf{v}, \tag{3.16}$$

$$l_2(w) = \int_\Omega h\, w, \tag{3.17}$$

$$l_3(\mathbf{s}) = -\int_{\Gamma_p} p_o \mathbf{s} \cdot \boldsymbol{\nu} + \int_\Omega \rho_f \mathbf{g} \cdot \mathbf{s}. \tag{3.18}$$

Our fully coupled finite element algorithm is based on the above variational formulation restricted to finite-dimensional spaces. First, let $\bar{\mathbf{u}}_d(t, \mathbf{x}) = \tilde{P}\mathbf{u}_d(t, \mathbf{x})$ and $\bar{\mathbf{z}}_d(t, \mathbf{x}) = \Pi_h \mathbf{z}_d(t, \mathbf{x})$. Then, the scheme becomes: find $\bar{\mathbf{u}} \in \bar{\mathbf{u}}_d + H^1([0, T]; \mathbf{V}_{h,0})$, $\bar{p} \in H^1([0, T]; W_h)$, and $\bar{\mathbf{z}} \in \bar{\mathbf{z}}_d + L^2([0, T]; \mathbf{S}_{h,0})$, such that

$$a_{\mathbf{u}}(\bar{\mathbf{u}}, \mathbf{v}) - \alpha(\nabla \cdot \mathbf{v}, \bar{p}) = l_1(\mathbf{v}), \tag{3.19}$$

$$(c_{\mathrm{o}} \bar{p}_{\mathrm{t}}, w) + \alpha(\nabla \cdot \bar{\mathbf{u}}_{\mathrm{t}}, w) + (\nabla \cdot \bar{\mathbf{z}}, w) = l_2(w), \tag{3.20}$$

$$(\tilde{\boldsymbol{\kappa}}^{-1} \bar{\mathbf{z}}, \mathbf{s}) - (\bar{p}, \nabla \cdot \mathbf{s}) = l_3(\mathbf{s}), \tag{3.21}$$

holds for every $t \in [0, T]$ and for all $(\mathbf{v}, w, \mathbf{s}) \in (\mathbf{V}_{h,0}, W_h, \mathbf{S}_{h,0})$. Additionally, we choose the following initial conditions for $\bar{\mathbf{u}}$ and $\bar{p}$:

$$a_{\mathbf{u}}(\bar{\mathbf{u}}, \mathbf{v})_{t=0} = a_{\mathbf{u}}(\mathbf{u}^o, \mathbf{v}), \quad \forall \mathbf{v} \in \mathbf{V}_h, \tag{3.22}$$

$$(\bar{p}, w)_{t=0} = (p^o, w), \quad \forall w \in W_h. \tag{3.23}$$

4 Existence and uniqueness

The existence and uniqueness of a solution of Eqs. 3.19–3.21 can be established. For uniqueness, assume that $(\bar{\mathbf{u}}_a, \bar{p}_a, \bar{\mathbf{z}}_a)$ and $(\bar{\mathbf{u}}_b, \bar{p}_b, \bar{\mathbf{z}}_b)$ are two solutions to Eqs. 3.19–3.21. Let $(\mathbf{e}_{\mathbf{u}}, e_p, \mathbf{e}_{\mathbf{z}})$ be the error between the two solutions. This error satisfies Eqs. 3.19–3.21 with null data, boundary and initial conditions. So take $\mathbf{v} = \frac{\partial}{\partial t}\mathbf{e}_{\mathbf{u}}$, $w = e_p$, and $\mathbf{s} = \mathbf{e}_{\mathbf{z}}$. By adding Eqs. 3.19 and 3.20 together, we have

$$a_{\mathbf{u}}\left(\mathbf{e}_{\mathbf{u}}, \frac{\partial}{\partial t}\mathbf{e}_{\mathbf{u}}\right) + c_{\mathrm{o}}\left(\frac{\partial}{\partial t} e_p, e_p\right) + (\nabla \cdot \mathbf{e}_{\mathbf{z}}, e_p) = 0. \tag{4.1}$$

Now, from Eq. 3.21, we see that

$$(\tilde{\boldsymbol{\kappa}}^{-1} \mathbf{e}_{\mathbf{z}}, \mathbf{e}_{\mathbf{z}}) = (\nabla \cdot \mathbf{e}_{\mathbf{z}}, e_p).$$

Substituting this into Eq. 4.1, and by using the chain rule from calculus, we see that

$$\frac{1}{2}\frac{\partial}{\partial t} a_{\mathbf{u}}(\mathbf{e}_{\mathbf{u}}, \mathbf{e}_{\mathbf{u}}) + \frac{1}{2} c_{\mathrm{o}} \frac{\partial}{\partial t}(e_p, e_p) + (\tilde{\boldsymbol{\kappa}}^{-1} \mathbf{e}_{\mathbf{z}}, \mathbf{e}_{\mathbf{z}}) = 0. \tag{4.2}$$

Integrating above equation from 0 to t, we arrive at the equation:

$$\frac{1}{2}[a_{\mathbf{u}}(\mathbf{e}_{\mathbf{u}}(t), \mathbf{e}_{\mathbf{u}}(t)) + c_{\mathrm{o}}(e_p(t), e_p(t))] - \frac{1}{2}\overbrace{[a_{\mathbf{u}}(\mathbf{e}_{\mathbf{u}}(0), \mathbf{e}_{\mathbf{u}}(0)) + c_{\mathrm{o}}(e_p(0), e_p(0))]}^{=0} + \int_0^t (\tilde{\boldsymbol{\kappa}}^{-1} \mathbf{e}_{\mathbf{z}}(\tau), \mathbf{e}_{\mathbf{z}}(\tau))\, \mathrm{d}\tau = 0.$$

Now, since the middle term vanishes by assumption, the above equation becomes

$$\frac{1}{2}[a_{\mathbf{u}}(\mathbf{e}_{\mathbf{u}}(t), \mathbf{e}_{\mathbf{u}}(t)) + c_{\mathrm{o}}(e_p(t), e_p(t))] + \int_0^t (\tilde{\boldsymbol{\kappa}}^{-1} \mathbf{e}_{\mathbf{z}}(\tau), \mathbf{e}_{\mathbf{z}}(\tau))\, \mathrm{d}\tau = 0.$$

Clearly, using the positive definiteness of $a_{\mathbf{u}}(\cdot, \cdot)$ and $\tilde{\boldsymbol{\kappa}}^{-1}$, we see that each term above must be zero. Thus, we conclude that $\mathbf{e}_{\mathbf{u}}(t) = e_p(t) = \mathbf{e}_{\mathbf{z}}(t) = 0$. Hence, $\bar{\mathbf{u}}_a(t) = \bar{\mathbf{u}}_b(t)$, $\bar{p}_a(t) = \bar{p}_b(t)$, and $\bar{\mathbf{z}}_a(t) = \bar{\mathbf{z}}_b(t)$ for each $t \geq 0$, thus establishing uniqueness.

To show existence, note that Eqs. 3.19 and 3.21 are algebraic equations relating $\bar{\mathbf{u}}$ to $\bar{p}$ and $\bar{\mathbf{z}}$ to $\bar{p}$, respectively. So, the strategy for proving existence is to rewrite Eq. 3.20 as a square system of ordinary linear differential equations for $\bar{p}$ in its finite element basis; thereafter, we can use ordinary differential equations (ODE) existence theory. To begin, we write the functions $\bar{\mathbf{u}}(t, \mathbf{x})$, $\bar{p}(t, \mathbf{x})$, and $\bar{\mathbf{z}}(t, \mathbf{x})$ as components in their respective finite element basis functions, $\mathbf{N}_{\mathbf{u}} = [N_{\mathbf{u},1}, \ldots, N_{\mathbf{u},n_{\mathbf{u}}}]$, $\mathbf{N}_p = [N_{p,1}, \ldots, N_{p,n_p}]$, and $\mathbf{N}_{\mathbf{z}} = [N_{\mathbf{z},1}, \ldots, N_{\mathbf{z},n_{\mathbf{z}}}]$:

$$\begin{aligned}
\bar{\mathbf{u}}(t, \mathbf{x}) &= \sum_j u_j(t) N_{\mathbf{u},j} + \sum_j u_{d,j}(t) N_{\mathbf{u},j}(\mathbf{x}) \\
&= \mathbf{u}_h(t, \mathbf{x}) \cdot \mathbf{N}_{\mathbf{u}}(\mathbf{x}) + \mathbf{u}_{dh}(t) \cdot \mathbf{N}_{\mathbf{u}}(\mathbf{x}), \\
\bar{p}(t, \mathbf{x}) &= \sum_j p_j(t) N_{p,j}(\mathbf{x}) \\
&= \mathbf{p}_h(t) \cdot \mathbf{N}_p(\mathbf{x}), \\
\bar{\mathbf{z}}(t, \mathbf{x}) &= \sum_j z_j(t) N_{\mathbf{z},j}(\mathbf{x}) + \sum_j z_{d,j}(t) N_{\mathbf{z},j}(\mathbf{x}) \\
&= \mathbf{z}_h(t) \cdot \mathbf{N}_{\mathbf{z}}(\mathbf{x}) + \mathbf{z}_{dh}(t) \cdot \mathbf{N}_{\mathbf{z}}(\mathbf{x}).
\end{aligned}$$

Here, $\mathbf{u}_h(t) = [u_1(t), \ldots, u_{n_{\mathbf{u}}}(t)]^{\mathrm{T}}$, $\mathbf{p}_h(t) = [p_1(t), \ldots, p_{n_p}(t)]^{\mathrm{T}}$, and $\mathbf{z}_h(t) = [z_1(t), \ldots, z_{n_{\mathbf{z}}}(t)]^{\mathrm{T}}$. The vectors $\mathbf{u}_{dh} = [u_{d,1}(t), \ldots, u_{d,n_{\mathbf{u}}}(t)]^T$, and $\mathbf{z}_{dh} = [z_{d,1}(t), \ldots, z_{d,n_{\mathbf{u}}}(t)]^T$ are the components of known functions $\bar{\mathbf{u}}_d$ and $\bar{\mathbf{z}}_d$, respectively, that come from the inhomogeneous essential conditions.

It is now instructive to rewrite Eqs. 3.19–3.21 in matrix form:

$$A_{\mathbf{uu}}\mathbf{u}_h - \alpha A_{p\mathbf{u}}\mathbf{p}_h = \mathbf{l}_1, \tag{4.3}$$

$$c_{\mathrm{o}} A_{pp}\frac{\partial \mathbf{p}_h}{\partial t} + \alpha A_{p\mathbf{u}}^{\mathrm{T}}\frac{\partial \mathbf{u}_h}{\partial t} + A_{\mathbf{z}p}\mathbf{z}_h = \mathbf{l}_2, \tag{4.4}$$

$$A_{\mathbf{zz}}\mathbf{z}_h - A_{\mathbf{z}p}^{\mathrm{T}}\mathbf{p}_h = \mathbf{l}_3. \tag{4.5}$$

We remark that the rhs vectors have been modified to include the effects of $\mathbf{u}_{dh}$ and $\mathbf{z}_{dh}$.

Now, we differentiate Eq. 4.3 with respect to time and solve for u_h to find

$$\frac{\partial \mathbf{u}_h}{\partial t} = A_{\mathbf{uu}}^{-1}\mathbf{l}_1' + \alpha A_{\mathbf{uu}}^{-1}A_{p\mathbf{u}}\frac{\partial \mathbf{p}_h}{\partial t}. \tag{4.6}$$

Here, $\mathbf{l}_1' \equiv \frac{\partial \mathbf{l}_1}{\partial t}$. Next, we use Eq. 4.5 to solve for $\mathbf{z}_h$:

$$\mathbf{z}_h = A_{\mathbf{zz}}^{-1}\mathbf{l}_3 + A_{\mathbf{zz}}^{-1}A_{\mathbf{z}p}^{\mathrm{T}}\mathbf{p}_h. \tag{4.7}$$

Then, plugging Eqs. 4.6 and 4.7 into Eq. 4.4, we have the following ODE:

$$\left(c_{\mathrm{o}}A_{pp} + \alpha A_{p\mathbf{u}}^{\mathrm{T}}A_{\mathbf{uu}}^{-1}A_{p\mathbf{u}}\right)\frac{\partial \mathbf{p}_h}{\partial t} = \mathbf{l}_2 - \alpha A_{p\mathbf{u}}^{T}A_{\mathbf{uu}}^{-1}\mathbf{l}_1' - A_{\mathbf{z}p}A_{\mathbf{zz}}^{-1}\mathbf{l}_3 - A_{\mathbf{z}p}A_{\mathbf{zz}}^{-1}A_{\mathbf{z}p}^{\mathrm{T}}\mathbf{p}_h.$$

The matrix multiplying $\frac{\partial \mathbf{p}_h}{\partial t}$ is the sum of a symmetric, positive-definite matrix A_{pp} and a symmetric, nonnegative definite[2] matrix $A_{p\mathbf{u}}^{\mathrm{T}}A_{\mathbf{uu}}^{-1}A_{p\mathbf{u}}$, and so is itself symmetric and positive definite. Therefore, given Eq. 2.2, its inverse can be taken. This property and the smoothness of the rhs (from the assumptions on the data) show that the ODE for $\mathbf{p}_h$ has a solution on $[0, T]$ [4]. In turn, given the nonsingularity of $A_{\mathbf{uu}}$ and $A_{\mathbf{zz}}$, respectively, $\mathbf{u}_h$ and $\mathbf{z}_h$ can be solved algebraically, thus establishing their existence.

5 Error estimates

We begin this section with a useful lemma regarding time derivatives;

Lemma 5.1 *Let B be a continuous linear operator defined on a Banach space X, and let $f : [0, T] \to X$ be continuously differentiable in time. Then, B and $\frac{\partial}{\partial t}$ are a commutative pair, that is, $B\frac{\partial f}{\partial t} = \frac{\partial}{\partial t}B(f)$.*

Remark 5.1 The above lemma is important when developing error estimates. In particular, we are interested in the cases $B = P_h$ or $B = \tilde{P}$.

[2]Indeed, it is positive definite provided one shows $A_{p\mathbf{u}}$ has full column rank.

For convenience, we now introduce some additional notation, in particular, the time-dependent auxiliary and projection errors, as:

$$E_p^A = P_h p - \bar{p}, \qquad E_p^I = p - P_h p,$$
$$E_{\mathbf{z}}^A = \Pi_h \mathbf{z} - \bar{\mathbf{z}}, \qquad E_{\mathbf{z}}^I = \mathbf{z} - \Pi_h \mathbf{z},$$
$$E_{\mathbf{u}}^A = \tilde{P}\mathbf{u} - \bar{\mathbf{u}}, \qquad E_{\mathbf{u}}^I = \mathbf{u} - \tilde{P}\mathbf{u}.$$

5.1 Continuous in time error estimates

Now, we examine a priori continuous time error estimates. We summarize our results in the following theorem:

Theorem 5.2 (Auxiliary error estimate) *Let r_1 be associated with the degree of the polynomials used in the mixed space $(W_h, \mathbf{S}_h)$ satisfying Eqs. 3.5a–3.5e, and let r_2 be the degree of the polynomials used in the displacement space $\mathbf{V}_h$ satisfying Eq. 3.6. Then, assuming sufficient regularity in the true solution, Eqs. 2.1 and 2.2,*

$$||E_{\mathbf{u}}^A||^2_{L^\infty(H^1)} + ||E_p^A||^2_{L^\infty(L^2)} + ||E_{\mathbf{z}}^A||^2_{L^2(L^2)} \le C(h^{2r_1+2} + h^{2r_2}), \tag{5.1}$$

where $C = C(T, \boldsymbol{\kappa}, c_{\mathrm{o}}, C_{\mathrm{coer}}, p, p_{\mathrm{t}}, \mathbf{z}, \mathbf{u}_{\mathrm{t}})$

Proof Here, for simplicity, we assume homogeneous essential conditions for the displacement and flux. We also assume $\alpha = 1$. Note that these assumptions affect the value of C in Eq. 5.1, but not the rate of convergence.

We denote by $(\bar{\mathbf{u}}, \bar{p}, \bar{\mathbf{z}})$ the approximate solution. Then, by Galerkin orthogonality, the following equations hold for all functions $(\mathbf{v}, w, \mathbf{s}) \in (\mathbf{V}_{h,0}, W_h, \mathbf{S}_{h,0})$:

$$a_{\mathbf{u}}(\mathbf{u} - \bar{\mathbf{u}}, \mathbf{v}) - (p - \bar{p}, \nabla \cdot \mathbf{v}) = 0, \tag{5.2}$$

$$(c_{\mathrm{o}}(p - \bar{p})_t + \nabla \cdot (\mathbf{u} - \bar{\mathbf{u}})_t, w) + (\nabla \cdot (\mathbf{z} - \bar{\mathbf{z}}), w) = 0, \tag{5.3}$$

$$(\tilde{\boldsymbol{\kappa}}^{-1}(\mathbf{z} - \bar{\mathbf{z}}), \mathbf{s}) - (p - \bar{p}, \nabla \cdot \mathbf{s}) = 0. \tag{5.4}$$

Now, by noting that $\mathbf{u} - \bar{\mathbf{u}} = E_{\mathbf{u}}^A + E_{\mathbf{u}}^I$, $p - \bar{p} = E_p^A + E_p^I$, and $\mathbf{z} - \bar{\mathbf{z}} = E_{\mathbf{z}}^A + E_{\mathbf{z}}^I$, and using the properties of

the above projections, we find that Eqs. 5.3 and 5.4 become:

$$c_o(E^A_{p\,t}, w) + \overbrace{c_o(E^I_{p_t}, w)}^{=0 \text{ by } L^2 \text{ proj.}} (\nabla \cdot E^A_{\mathbf{u}\,t}, w) + (\nabla \cdot E^I_{\mathbf{u}t}, w) \times (\nabla \cdot E^A_{\mathbf{z}}, w) + \overbrace{(\nabla \cdot E^I_{\mathbf{z}}, w)}^{=0 \text{ by Eq. (3.5a)}} = 0, \tag{5.5}$$

$$(\tilde{\boldsymbol{\kappa}}^{-1} E^A_{\mathbf{z}}, \mathbf{s}) + (\tilde{\boldsymbol{\kappa}}^{-1} E^I_{\mathbf{z}}, \mathbf{s}) - (E^A_p, \nabla \cdot \mathbf{s}) - \overbrace{(E^I_p, \nabla \cdot \mathbf{s})}^{=0 \text{ by Eq. (3.5d)}} = 0. \tag{5.6}$$

Then, letting $w = E^A_p$ and $\mathbf{s} = E^A_{\mathbf{z}}$ in Eqs. 5.5 and 5.6, after summing the non-zero terms in the above two equations and using the chain rule (in time), we find that, after some rearrangement,

$$\frac{1}{2} c_o \frac{\partial}{\partial t}(E^A_p, E^A_p) + (\nabla \cdot E^A_{\mathbf{u}\,t}, E^A_p) + (\tilde{\boldsymbol{\kappa}}^{-1} E^A_{\mathbf{z}}, E^A_{\mathbf{z}}) = -(\tilde{\boldsymbol{\kappa}}^{-1} E^I_{\mathbf{z}}, E^A_{\mathbf{z}}) - (\nabla \cdot E^I_{\mathbf{u}t}, E^A_p). \tag{5.7}$$

Next, we set $\mathbf{v} = E^A_{\mathbf{u}\,t}$ in Eq. 5.2. Then, by using the symmetry of $a_{\mathbf{u}}$ and the chain rule (in time), we find that

$$\frac{1}{2} \frac{\partial}{\partial t} a_{\mathbf{u}}(E^A_{\mathbf{u}}, E^A_{\mathbf{u}}) + \overbrace{a_{\mathbf{u}}(E^I_{\mathbf{u}}, E^A_{\mathbf{u}\,t})}^{=0 \text{ by Elliptic proj.}} - (E^A_p, \nabla \cdot E^A_{\mathbf{u}\,t}) - (E^I_p, \nabla \cdot E^A_{\mathbf{u}\,t}) = 0. \tag{5.8}$$

If we then sum Eqs. 5.7 and 5.8, integrate from 0 to T, and use Eqs. 3.22 and 3.23 to see that $a_{\mathbf{u}}(E^A_{\mathbf{u}}, E^A_{\mathbf{u}})|_{t=0} = 0$ and $(E^A_p, E^A_p)|_{t=0} = 0$, we deduce a formula for the auxiliary error,

$$\frac{1}{2}[a_{\mathbf{u}}(E^A_{\mathbf{u}}, E^A_{\mathbf{u}}) + c_o(E^A_p, E^A_p)]|_{t=T} + \int_0^T (\tilde{\boldsymbol{\kappa}}^{-1} E^A_{\mathbf{z}}(\tau), E^A_{\mathbf{z}}(\tau)\, d\tau = \Phi_1 + \Phi_2 + \Phi_3, \tag{5.9}$$

where

$$\Phi_1 = -\int_0^T (\tilde{\boldsymbol{\kappa}}^{-1} E^I_{\mathbf{z}}(\tau), E^A_{\mathbf{z}}(\tau))\, d\tau, \tag{5.10}$$

$$\Phi_2 = -\int_0^T (\nabla \cdot E^I_{\mathbf{u}t}(\tau), E^A_p(\tau))\, d\tau, \tag{5.11}$$

$$\Phi_3 = \int_0^T (E^I_p(\tau), \nabla \cdot E^A_{\mathbf{u}\,t}(\tau))\, d\tau. \tag{5.12}$$

To bound the above quantities, we make use primarily of the Cauchy–Schwarz and Young inequalities (i.e., for $a, b \geq 0, \epsilon \geq 0, ab \leq \frac{1}{2\epsilon} a^2 + \frac{\epsilon}{2} b^2$):

$$\begin{aligned}
\Phi_1 &= -\int_0^T (\tilde{\boldsymbol{\kappa}}^{-1} E^I_{\mathbf{z}}(\tau), E^A_{\mathbf{z}}(\tau))\, d\tau \\
&\leq \int_0^T ||\tilde{\boldsymbol{\kappa}}^{-1} E^I_{\mathbf{z}}(\tau)||_0 ||E^A_{\mathbf{z}}(\tau)||_0\, d\tau \\
&\leq C \int_0^T ||\tilde{\boldsymbol{\kappa}}^{-1} E^I_{\mathbf{z}}(\tau)||_0^2\, d\tau + \epsilon \int_0^T ||E^A_{\mathbf{z}}(\tau)||_0^2\, d\tau \\
&\leq \frac{C}{\lambda^2_{\min}} \int_0^T ||E^I_{\mathbf{z}}(\tau)||_0^2\, d\tau + \epsilon \int_0^T ||E^A_{\mathbf{z}}(\tau)||_0^2\, d\tau.
\end{aligned}$$

$$\begin{aligned}
\Phi_2 &= -\int_0^T (\nabla \cdot E^I_{\mathbf{u}t}(\tau), E^A_p(\tau))\, d\tau \\
&\leq \int_0^T ||\nabla \cdot E^I_{\mathbf{u}t}(\tau)||_0 ||E^A_p(\tau)||_0\, d\tau \\
&\leq \frac{1}{2} \int_0^T ||\nabla \cdot E^I_{\mathbf{u}t}(\tau)||_0^2\, d\tau + \frac{1}{2} \int_0^T ||E^A_p(\tau)||_0^2\, d\tau \\
&\leq \frac{1}{2} \int_0^T ||E^I_{\mathbf{u}t}(\tau)||_1^2\, d\tau + \frac{1}{2} \int_0^T ||E^A_p(\tau)||_0^2\, d\tau.
\end{aligned}$$

To bound Φ_3, we first integrate by parts and remember that $||\nabla \cdot E^A_{\mathbf{u}}(0)|| = 0$:

$$\begin{aligned}
\Phi_3 &= \int_0^T (E^I_p(\tau), \nabla \cdot E^A_{\mathbf{u}\,t}(\tau))\, d\tau \\
&= -\int_0^T (E^I_{p_t}(\tau), \nabla \cdot E^A_{\mathbf{u}}(\tau))\, d\tau + (E^I_p, \nabla \cdot E^A_{\mathbf{u}})|_0^T \\
&\leq \int_0^T ||E^I_{p_t}(\tau)||_0 ||\nabla \cdot E^A_{\mathbf{u}}(\tau)||_0\, d\tau \\
&\quad + ||E^I_p(T)||_0 ||\nabla \cdot E^A_{\mathbf{u}}(T)||_0 \\
&\leq \frac{1}{2} \int_0^T ||E^I_{p_t}(\tau)||_0^2\, d\tau + \frac{1}{2} \int_0^T ||E^A_{\mathbf{u}}(\tau)||_1^2\, d\tau \\
&\quad + C||E^I_p(T)||_0^2 + \epsilon ||E^A_{\mathbf{u}}(T)||_1^2.
\end{aligned}$$

We now use the above bounds on $\Phi_1 - \Phi_3$ in Eq. 5.9; in addition, we use the inequalities $a_{\mathbf{u}}(E^A_{\mathbf{u}}, E^A_{\mathbf{u}}) \geq C_{\text{coer}} ||E^A_{\mathbf{u}}||_1^2$ (coercivity) and $(\tilde{\boldsymbol{\kappa}}^{-1} E^A_{\mathbf{z}}, E^A_{\mathbf{z}}) \geq$

$\frac{1}{\lambda_{\max}}||E^A_{\mathbf{z}}||^2_0$ (boundedness of $\boldsymbol{\kappa}$). So, after rearrangement, we find:

$$\begin{aligned}
&\Big(\frac{1}{2}C_{\text{coer}} - \epsilon\Big)||E^A_{\mathbf{u}}(T)||^2_1 + \frac{1}{2}c_{\text{o}}||E^A_p(T)||^2_0 \\
&\quad + \Big(\frac{1}{\lambda_{\max}} - \epsilon\Big)\int_0^T ||E^A_{\mathbf{z}}(\tau)||^2_0\,\mathrm{d}\tau \\
&\quad \le \frac{1}{2}\Big[\int_0^T ||E^A_p(\tau)||^2_0\,\mathrm{d}\tau + \int_0^T ||E^A_{\mathbf{u}}(\tau)||^2_1\,\mathrm{d}\tau\Big] \\
&\qquad + C\Big[||E^I_p(T)||^2_0 + \frac{1}{\lambda^2_{\min}}\int_0^T ||E^I_{\mathbf{z}}(\tau)||^2_0\,\mathrm{d}\tau \\
&\qquad\quad + \int_0^T ||E^I_{\mathbf{u}_t}(\tau)||^2_1\,\mathrm{d}\tau + \int_0^T ||E^I_{p_t}(\tau)||^2_0\,\mathrm{d}\tau\Big],
\end{aligned}$$

where[3] ϵ and C are independent of T and h. Then, provided that ϵ is small enough so that the lhs coefficients are all positive, we may preserve the inequality by setting each coefficient on the lhs to equal the smallest of the terms. After dividing the equation by that term, we find the inequality,

$$\begin{aligned}
&||E^A_{\mathbf{u}}(T)||^2_1 + ||E^A_p(T)||^2_0 + \int_0^T ||E^A_{\mathbf{z}}(\tau)||^2_0\,\mathrm{d}\tau \\
&\quad \le C(\boldsymbol{\kappa}, c_{\text{o}}, C_{\text{coer}})\Big[\int_0^T ||E^A_p(\tau)||^2_0\,\mathrm{d}\tau \\
&\qquad\qquad + \int_0^T ||E^A_{\mathbf{u}}(\tau)||^2_1\,\mathrm{d}\tau\Big] \\
&\qquad + C(\boldsymbol{\kappa}, c_{\text{o}}, C_{\text{coer}})\Big[||E^I_p(T)||^2_0 + \int_0^T ||E^I_{\mathbf{z}}(\tau)||^2_0\,\mathrm{d}\tau \\
&\qquad\qquad + \int_0^T ||E^I_{\mathbf{u}_t}(\tau)||^2_1\,\mathrm{d}\tau \\
&\qquad\qquad + \int_0^T ||E^I_{p_t}(\tau)||^2_0\,\mathrm{d}\tau\Big].
\end{aligned}$$

Using Gronwall's inequality (see [8]),

$$\begin{aligned}
&||E^A_{\mathbf{u}}(T)||^2_1 + ||E^A_p(T)||^2_0 + \int_0^T ||E^A_{\mathbf{z}}(\tau)||^2\,\mathrm{d}\tau \\
&\quad \le C(T, \boldsymbol{\kappa}, c_{\text{o}}, C_{\text{coer}})\Big[||E^I_p(T)||^2_0 + \int_0^T ||E^I_{\mathbf{z}}(\tau)||^2_0\,\mathrm{d}\tau \\
&\qquad + \int_0^T ||E^I_{\mathbf{u}_t}(\tau)||^2_1\,\mathrm{d}\tau + \int_0^T ||E^I_{p_t}(\tau)||^2_0\,\mathrm{d}\tau\Big].
\end{aligned}$$

[3] We remark that each ϵ can be chosen independently.

We note that the above estimate is true for all $0 \le T$. If, in addition, we apply the appropriate approximation properties, we deduce

$$\begin{aligned}
&\sup_{0\le\tau\le T} ||E^A_{\mathbf{u}}(\tau)||^2_1 + \sup_{0\le\tau\le T} ||E^A_p(\tau)||^2_0 + \int_0^T ||E^A_{\mathbf{z}}(\tau)||^2_0\,\mathrm{d}\tau \\
&\quad \le C(T, \boldsymbol{\kappa}, c_{\text{o}}, C_{\text{coer}})\Big[h^{2r_1+2}\sup_{0\le\tau\le T} ||p(\tau)||^2_{r_1+1} \\
&\qquad\qquad + h^{2r_1+2}\int_0^T ||z(\tau)||^2_{r_1+1}\,\mathrm{d}\tau \\
&\qquad\qquad + h^{2r_2}\int_0^T ||\mathbf{u}_t(\tau)||^2_{r_2+1}\,\mathrm{d}\tau \\
&\qquad\qquad + h^{2r_1+2}\int_0^T ||p_t(\tau)||^2_{r_1+1}\,\mathrm{d}\tau\Big].
\end{aligned}$$

Or, using standard nomenclature,

$$\begin{aligned}
&||E^A_{\mathbf{u}}||^2_{L^\infty(H^1)} + ||E^A_p||^2_{L^\infty(L^2)} + ||E^A_{\mathbf{z}}||^2_{L^2(L^2)} \\
&\quad \le C(T, \boldsymbol{\kappa}, c_{\text{o}}, C_{\text{coer}}, p, p_{,t}, \mathbf{z}, \mathbf{u}_{,t})(h^{2r_1+2} + h^{2r_2}).
\end{aligned}$$

□

The importance of auxiliary error estimates is found when coupled with the triangle inequality and is summarized in the following corollary:

Corollary 5.3 (Finite element error estimate) *With the same conditions as in the preceding theorem, the following finite element error estimate holds:*

$$\begin{aligned}
&||\mathbf{u} - \bar{\mathbf{u}}||^2_{L^\infty(H^1)} + ||p - \bar{p}||^2_{L^\infty(L^2)} + ||\mathbf{z} - \bar{\mathbf{z}}||^2_{L^2(L^2)} \\
&\quad \le C(T, \boldsymbol{\kappa}, c_{\text{o}}, C_{\text{coer}}, p, p_{,t}, \mathbf{z}, \mathbf{u}_{,t})(h^{2r_1+2} + h^{2r_2}).
\end{aligned} \tag{5.13}$$

Proof Applying the triangle inequality to the lhs of Eq. 5.13 yields:

$$\begin{aligned}
&||\,\mathbf{u} - \bar{\mathbf{u}}||^2_{L^\infty(H^1)} + ||p - \bar{p}||^2_{L^\infty(L^2)} + ||\mathbf{z} - \bar{\mathbf{z}}||^2_{L^2(L^2)} \\
&\quad \le \overbrace{||E^A_{\mathbf{u}}||^2_{L^\infty(H^1)} + ||E^A_p||^2_{L^\infty(L^2)} + ||E^A_{\mathbf{z}}||^2_{L^2(L^2)}}^{\text{Auxiliary error}} \\
&\qquad + \overbrace{||E^I_{\mathbf{u}}||^2_{L^\infty(H^1)} + ||E^I_p||^2_{L^\infty(L^2)} + ||E^I_{\mathbf{z}}||^2_{L^2(L^2)}}^{\text{Interpolation error}}.
\end{aligned}$$

Use of interpolation estimates and the theorem on auxiliary estimates concludes the corollary. □

6 Numerical results

The equations governing poroelasticity form a complicated coupled system of partial differential equations, and hence, there are very few analytical solutions available. However, there are some known solutions that provide an ideal opportunity to examine the numerical accuracy of the algorithms presented herein. In this paper, we turn to the well-known case of Mandel's problem. This problem gives us a chance to test our algorithm in a two-dimensional setting, and it also provides a nice example of the dynamics involved in a fluid–solid interaction.

6.1 Mandel's problem

Mandel's problem is important because it admits an analytical solution in two dimensions on a finite domain. The original paper by Mandel [19] presented only an analytical form for the pressure; later, Abousleiman [1] extended the results to include analytical expressions for the displacement and stress. It is therefore an excellent model to verify the accuracy of a poroelasticity algorithm. Mandel's problem is also fascinating from the point of view that it clearly illustrates that solid–fluid interactions can lead to unexpected behavior, and thus highlights the need for poroelasticity theory in practice.

For a precise formulation of the problem, we consider a poroelastic slab of extent $2a$ in the x direction, $2b$ in the y direction, and infinitely long in the z direction. The slab is sandwiched in between two rigid plates as shown in Fig. 1. At time $t = 0$, a downward surface force of magnitude $2F$ is applied to the top plate, and an equal but upward force is applied to the bottom plate. Because the plates are considered rigid, we must impose the additional constraint that the vertical displacements at the top and bottom, respectively, are uniform. This requirement ensures that the slab remains in contact with the plates. We incorporate this constraint into our methods by use of Lagrange multipliers. In addition, at all times, the slab at $x = \pm a$ remains drained, thus leading to the boundary condition $p(\pm a, y, t) = 0$.

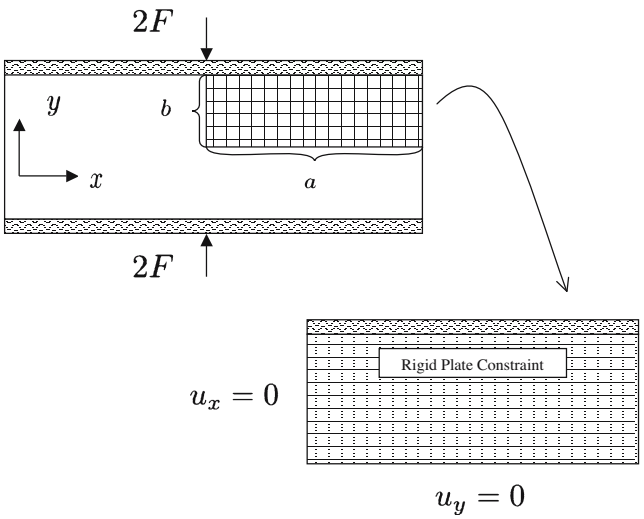

Fig. 1 Mandel's problem

The application of a load causes an instantaneous and uniform pressure increase throughout the domain; the theory predicts this to be $p^+ \equiv \lim_{t\to 0} p(\mathbf{x}, t) = \frac{1}{3a} B(1 + \nu_u) F$. Also, the x displacement depends only on x and t, and the y displacement depends on y and t. We can thus define the following x and y settlements: $s_x(t) = u_x(x = a, t)$ and $s_y = u_y(y = b, t)$. It is predicted that there will be instantaneous and asymptotic settlements,

$$s_{xo} \equiv \lim_{t\to 0} s_x(t) = \frac{F\nu_u}{2\mu},$$

$$s_{x\infty} \equiv \lim_{t\to \infty} s_x(t) = \frac{F\nu}{2\mu},$$

$$s_{yo} \equiv \lim_{t\to 0} s_y(t) = \frac{-F(1-\nu_u)b}{2\mu a},$$

$$s_{y\infty} \equiv \lim_{t\to \infty} s_y(t) = \frac{-F(1-\nu)b}{2\mu a}.$$

At this point, it is useful to remark that the problem is symmetric about the x and the y axes, and is independent of the z direction. Therefore, we may reduce the computational domain to only the upper-right quadrant of the xy plane, as illustrated in Fig. 1. Thus, we add to the governing equations 2.3a and 2.3b the following boundary and initial conditions on the domain $(0, a) \times (0, b)$:

$$u_x = 0, \quad x = 0;$$

$$u_y = 0, \quad y = 0;$$

$$\mathbf{t}_N \cdot \boldsymbol{\nu} = -2F, \quad y = b, \quad = 0 \text{ otherwise};$$

$$p = 0, \quad x = a;$$

$$-\frac{1}{\mu_f} \boldsymbol{\kappa} \nabla p \cdot \boldsymbol{\nu} = 0, \quad x = 0, \quad y = 0, \quad y = b;$$

$$u_y(x, y = b) = \text{constant} \ \text{(Rigid Plate Constraint)};$$

$$p = \mathbf{u} = 0, \quad t = 0;$$

We also remark that the constant in the rigid plate constraint is time-dependent.

We refer now to the notation in Appendix A1 as we list the analytical series solutions for the pressure, displacement, and stress as found in Abousleiman [1]:

$$p = \frac{2FB(1+\nu_u)}{3a}\sum_{n=1}^{\infty}\frac{\sin\alpha_n}{\alpha_n-\sin\alpha_n\cos\alpha_n}\times\left(\cos\frac{\alpha_n x}{a}-\cos\alpha_n\right)\exp(-\alpha_n^2 c_f t/a^2),$$

$$u_x = \left[\frac{F\nu}{2\mu a}-\frac{F\nu_u}{\mu a}\sum_{n=1}^{\infty}\frac{\sin\alpha_n\cos\alpha_n}{\alpha_n-\sin\alpha_n\cos\alpha_n}\times\exp(-\alpha_n^2 c_f t/a^2)\right]x + \frac{F}{\mu}\sum_{n=1}^{\infty}\frac{\cos\alpha_n}{\alpha_n-\sin\alpha_n\cos\alpha_n}\sin\frac{\alpha_n x}{a}\exp(-\alpha_n^2 c_f t/a^2),$$

$$u_y = \left[\frac{-F(1-\nu)}{2\mu a}+\frac{F(1-\nu_u)}{\mu a}\sum_{n=1}^{\infty}\frac{\sin\alpha_n\cos\alpha_n}{\alpha_n-\sin\alpha_n\cos\alpha_n}\times\exp(-\alpha_n^2 c_f t/a^2)\right]y,$$

$$\sigma_{yy} = -\frac{F}{a}-\frac{2FB(\nu_u-\nu)}{a(1-\nu)}\sum_{n=1}^{\infty}\frac{\sin\alpha_n}{\alpha_n-\sin\alpha_n\cos\alpha_n}\times\cos\frac{\alpha_n x}{a}\exp(-\alpha_n^2 c_f t/a^2) + \frac{2F}{a}\sum_{n=1}^{\infty}\frac{\sin\alpha_n\cos\alpha_n}{\alpha_n-\sin\alpha_n\cos\alpha_n}\exp(-\alpha_n^2 c_f t/a^2).$$

We note that all other components of the stress tensor are zero, $\sigma_{xx}=\sigma_{xy}=0$. We note that, for the above equations, α_n represents the positive solutions to the nonlinear equation

$$\tan\alpha_n = \frac{1-\nu}{\nu_u-\nu}\alpha_n,$$

and must be solved for numerically.

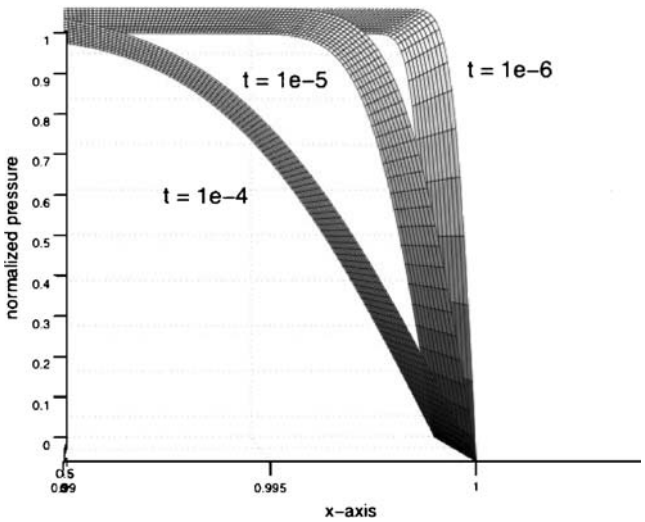

Fig. 2 Mandel's pressure solution and boundary layer as $t \to 0$

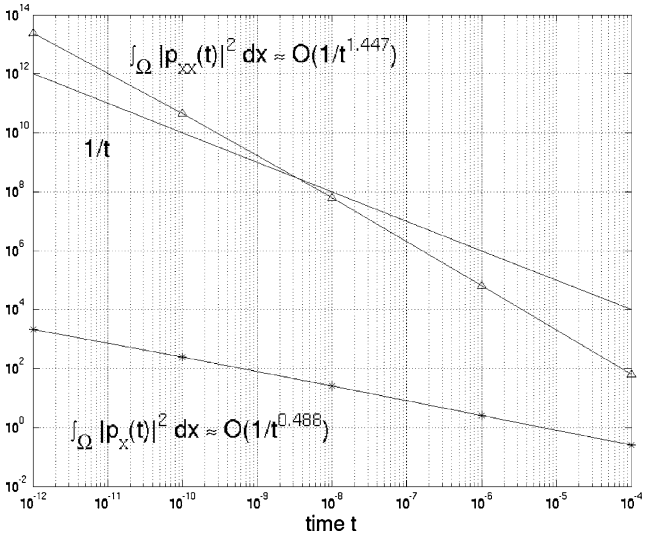

Fig. 3 Mandel's problem. The pressure integrals $||p_x(t)||_0^2$ and $||p_{xx}(t)||_0^2$

6.1.1 Results

Recall that the optimal error estimates presented herein stipulate a *sufficiently smooth* analytical solution. However, full-order convergence for even the lowest-order methods requires that $p \in L^2(H^2)$. One can see why by examining the proof of the error estimates given earlier. Assuming sufficient regularity implied that the following integrals are finite:

$$\int_0^T ||E_{\mathbf{z}}^I(\tau)||_0^1 d\tau \le h^{2k+2}\int_0^T ||\mathbf{z}(\tau)||_{k+1}^2 d\tau < \infty,$$

where k is the order of the mixed space. However, even for $k=0$, if $p \notin L^2(H^2)$, then $\int_0^T ||\mathbf{z}(\tau)||_1^2 d\tau = \infty$.

Indeed, for Mandel's problem, Fig. 2 shows the true pressure solution for a typical choice of physical parameters. As $t \to 0$, a very large gradient occurs. Naturally, this leads one to suspect that the regularity of the pressure might be limited. This is confirmed by looking at Fig. 3, which shows the regularity of the pressure by computing $||p_x(t)||_0^2$ and $||p_{xx}(t)||_0^2$. It is discovered that

$$||p_x(t)||_0^2 \approx O(t^{-0.488}) \tag{6.1}$$

$$||p_{xx}(t)||_0^2 \approx O(t^{-1.447}) \tag{6.2}$$

The order approximation (6.1) implies that $p \in L^2(H^1)$, but Eq. 6.2 shows that $p \notin L^2(H^2)$.

Thus, it is reasonable to assume that $p \in L^2(H^{1+s})$ for some $s \in [0, 1)$. Furthermore, it is precisely this value of s that limits the best rate of convergence that one might expect from the CG/Mixed algorithm for Mandel's problem.

For numerical verification of our algorithms, we use a force $F = 2,000$. Standard continuous linear elements are used to approximate the displacement, and the lowest Raviart–Thomas space is used for the flow variables. The backward Euler scheme is used. The top image in Fig. 4 shows how the computed pressure error, $||p - \bar{p}||_{L^\infty(L^2)}$, varies with element size h. The bottom image shows the displacement error, $||\mathbf{u} - \bar{\mathbf{u}}||_{L^\infty(H^1)}$. To minimize the effects of the error produced by the time discretization, a small time step of $\Delta t = 1e-6$ is chosen. The convergence rate is determined by the slope of the logarithm of the error (≈ 0.500117).

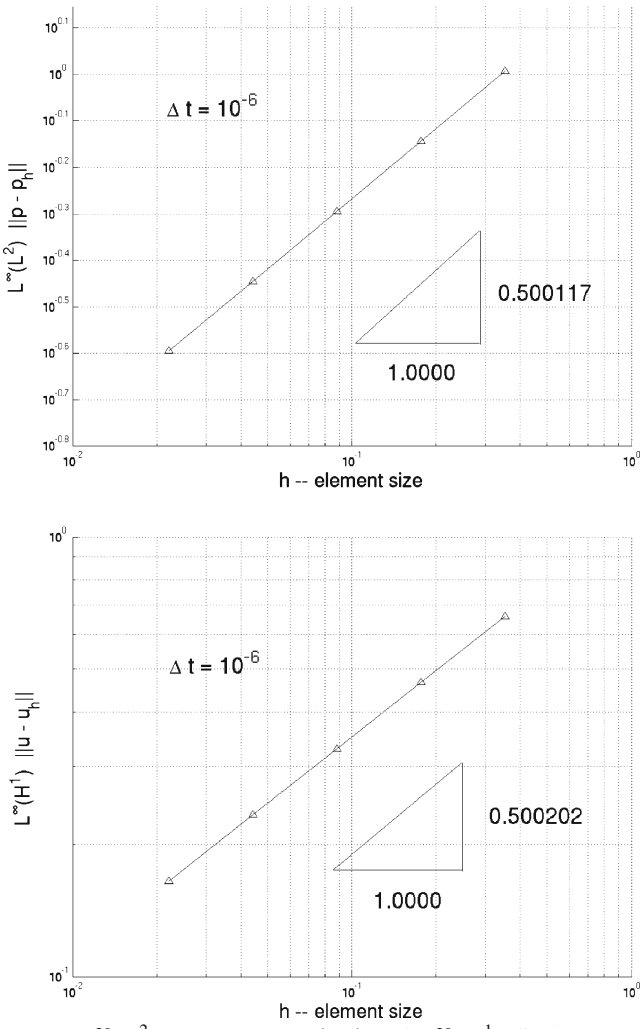

Fig. 4 $L^\infty(L^2)$ pressure error (*top*) and $L^\infty(H^1)$ displacement error (*bottom*) in Mandel's problem

The convergence rate (≈ 0.5) for both the pressure and displacement conforms to the expectation that the lack of regularity in the pressure solution would degrade performance. From the convergence rate and the theorem on error estimates, one might be led to conclude that $p \in L^2(H^{\frac{3}{2}\pm\epsilon})$ for some small $0 \leq \epsilon << 1$.

For a larger time step, the finite element solution might exhibit a better convergence rate because the large pressure gradient subsides over time. However, the time-discretization error can become problematic for those larger time steps. See Phillips and Wheeler [22] for the analysis of the discrete-in-time case and an example using Terzaghi's consolidation problem, which has a pressure solution profile similar to that for Mandel's problem.

An interesting aspect of Mandel's problem is shown in Fig. 5 – the increase in pressure (above the initial increase) near the center of the medium. This is known as the *Mandel–Creyer* effect and is a phenomenon particular to poroelastic material. The increase occurs because the deformation and rigid plate condition create an effect similar to that of a source term in the pressure equation. Indeed, Coussy [6] shows that one can reduce the diffusion equation to one involving the normalized pressure and a source as

$$\frac{\partial \hat{p}}{\partial \hat{t}} - \frac{\partial^2 \hat{p}}{\partial \hat{x}^2} = 2\sum_{n=1}^{\infty} \frac{\alpha_n^2 \sin\alpha_n \cos\alpha_n}{\alpha_n - \sin\alpha_n \cos\alpha_n} \exp(-\alpha_n^2 \hat{t}). \qquad (6.3)$$

The source term is time-dependent only (independent of $\mathbf{x}$), and it can be quite large at early times. The interesting behavior has been confirmed experimentally in the work of Gibson et al. [11] and Verruijt [32].

Appendix A1: Additional notation and terms in the literature

For completeness, we present here some additional terms and notations commonly found in poroelastic literature. Though not essential for the development of our model and the subsequent error estimates, familiarity with this additional nomenclature will be helpful when discussing numerical results.

The first of the additional terms can be written in terms of the Lamé coefficients μ and λ and are common in the field of linear elasticity. They are, respectively,

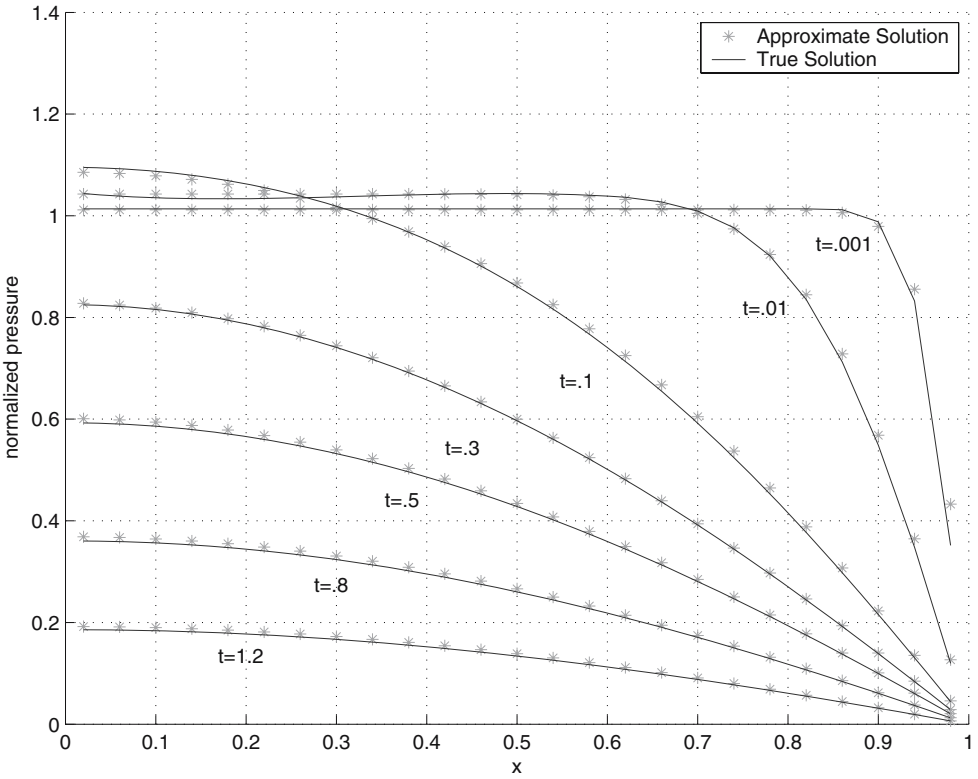

Fig. 5 The Mandel–Creyer effect is captured by the approximate solution

the *skeleton bulk modulus* K, *Young's modulus* E, and *Poisson's coefficient* ν:

$$K = \lambda + \frac{2}{3}\mu,$$
$$E = \mu\frac{9K}{3K+\mu},$$
$$\nu = \frac{3K-2\mu}{2(3K+\mu)}.$$

There are also "undrained" versions of the above coefficients and are denoted by the subscript u: K_u, E_u, ν_u. Additionally, K_u has the following relation,

$$K_\mathrm{u} = K + \frac{\alpha^2}{c_\mathrm{o}}.$$

With the above, two useful terms have been defined: the *fluid diffusivity coefficient* c_f and *Skempton's coefficient* B:

$$c_\mathrm{f} = \frac{1}{c_\mathrm{o}}\boldsymbol{\kappa}\frac{K+\frac{4}{3}\mu}{K_\mathrm{u}+\frac{4}{3}\mu},$$
$$B = \frac{\alpha}{c_\mathrm{o}K_\mathrm{u}}.$$

Clearly, c_f is usefully defined only for the case where the permeability $\boldsymbol{\kappa}$ is a constant. Skempton's coefficient can be used to reveal a useful relation between Poisson's coefficient and its undrained version,

$$\frac{\alpha B(1-2\nu)}{3} = \frac{\nu_\mathrm{u}-\nu}{1+2\nu_\mathrm{u}}.$$

References

1. Abousleiman, Y., Cheng, A.-D., Cui, L., Detournay, E., Roegiers, J.: Mandel's problem revisited. Géotechnique **46**, 187–195 (1996)
2. Biot, M.: General theory of three-dimensional consolidation. J. Appl. Phys. **2**, 155–164 (1941)
3. Biot, M.: Theory of elasticity and consolidation for a porous anisotropic media. J. Appl. Phys. **26**(2), 182–185 (1955)
4. Boyce, W., DiPrima, R.: Elementary Differential Equations, 7th edn. Wiley, New York (2001)
5. Brenner, S., Scott, L.: The Mathematical Theory of Finite Element Methods. Springer, Berlin Heidelberg New York (1994)
6. Coussy, O.: Poromechanics. Wiley, New York (2004)
7. Detournay, E., Cheng, A.-D.: Poroelastic response of a borehole in non-hydrostatic stress field. Int. J. Rock Mech. Mining Sci. **25**, 171–182 (1988)
8. Evans, L.: Partial Differential Equations. American Mathematical Society, Providence (1998)
9. Gai, X.: A Coupled Geomechanics and Reservoir Flow Model on Parallel Computers. Ph.D. thesis, University of Texas at Austin (2004)
10. Garagash, D., Detournay, E.: An analysis of the influence of the pressurization rate on the borehole breakdown pressure. J. Solids Struct. **34**(2), 3099–3118 (1997)

11. Gibson, R., Knight, K., Taylor, P.: A critical experiment to examine theories of three-dimensional consolidation. Eur. Conf. Soil Mech. **1**, 69–73 (1963)
12. Hudson, J., Stephansson, O., Andersson, J., Tsang, C.-F., Ling, L.: Coupled T-H-M issues related to radioactive waste repository design and performance. Int. J. Rock Mech. Mining Sci. **38**, 143–161 (2001)
13. Kim, J.-M., Parizek, R.: Numerical simulation of the noordbergum effect resulting from groundwater pumping in a layered aquifer system. J. Hydrol. **202**, 231–243 (1997)
14. Langford, T.: Northwest Houston Sinking Faster than Coastal Areas. http://www.Reporter-News.com (1997)
15. Lewis, R.W., Schrefler, B.A.: The Finite Element Method in the Deformation and Consolidation of Porous Media. Wiley & Sons, Chichester (1987)
16. Lin, J.: An Interview with Jian Lin, Ph.D. http://www.esi-topics.com/earthquakes/interviews/JianLin.html (2003)
17. Liu, R.: Discontinuous Galerkin finite element solution for poromechanics. Ph.D. thesis, University of Texas at Austin (2004)
18. Lubick, N.: Modeling complex, multiphase porous media systems. SIAM News **5**(3) (2002)
19. Mandel, J.: Consolidation des sols (étude mathématique). Géotechnique **30**, 287–299 (1953)
20. Nedelec, J.: Mixed finite elements in $\mathbb{R}^3$. Numer. Math. **35**, 315–341 (1980)
21. Phillips, P.J.: Finite element methods for linear poroelasticity: theoretical and computational results. Ph.D. thesis, University of Texas at Austin (2005)
22. Phillips, P.J., Wheeler, M.F. : A coupling of mixed and continuous Galerkin finite element methods for poroelasticity II: the discrete-in-time case. Comput. Geosci. doi:10.1007/s10596-007-9044-z
23. Rajapakse, R.: Stress analysis of borehole in poroelastic medium. J. Eng. Mech. **119**(6), 1205–1227 (1993)
24. Raviart, R.A, Thomas, J.W.: A mixed finite element method for 2nd order elliptic problems. In: Mathematical Aspects of the Finite Element Method. Lecture Notes in Mathematics, vol. 606, pp. 292–315. Springer, Berlin Heidelberg New York (1977)
25. Rivière, B., Wheeler, M.: Optimal error estimates applied to linear elasticity. Technical report, ICES Report. ICES, Austin (2000)
26. Roose, T., Netti, P., Munn, L., Boucher, Y., Jain, R.: Solid stress generated by spheroid growth estimated using a linear poroelastic model. Microvasc. Res. **66**, 204–212 (2003)
27. Rutqvist, J., Tsang, C.-F.: Analysis of thermal–hydrologic–mechanical behavior near an emplacement drift at Yucca mountain. J. Contam. Hydrol. **62–63**, 637–652 (2003)
28. Showalter, R.E.: Diffusion in poro-elastic media. J. Math. Anal. Appl. **251**, 310–340 (2000)
29. Smillie, A., Sobey, I., Molnar, Z.: A hydro-elastic model of hydrocephalus. Technical report, Oxford University Computing Laboratory: Numerical Analysis Group, Oxford (2004)
30. Swan, C., Lakes, R., Brand, R., Stewart, K.: Micromechanically based poroelastic modeling of fluid flow in Haversian bone. J. Biomech. Eng. **125**(1), 25–37 (2003)
31. Terzaghi, K.: Theoretical Soil Mechanics. Wiley, New York (1943)
32. Verruijt, A.: Discussion. Proc. 6th Int. Conf. Soil Mech. **3**, 401–402 (1965)
33. Wang, H.F.: Theory of Linear Poroelasticity with Applications to Geomechanics and Hydrogeology. Princeton University Press, Princeton (2000)
34. Wang, Y., Dusseault, M.: A coupled conductive-convective thermo-poroelastic solution and implications for wellbore stability. J. Petrol. Sci. Eng. **38**, 187–198 (2003)
35. Weiser, A., Wheeler, M.: On convergence of block-centered finite differences and elliptic equations. SIAM J. Numer. Anal. **251**(2), 351–375 (1988)
36. Wheeler, M.F.: A priori L^2 error estimates for Galerkin approximations to parabolic partial differential equations. SIAM J. Numer. Anal. **10**, 723–759 (1973)
37. Wheeler, M.F., Phillips, P.J.: A coupling of mixed and Galerkin methods for poro-elasticity. In: Proceedings of the Second MIT Conference on Computational Fluid and Solid Mechanics, MIT, Cambridge, 17–20 June 2003
38. Zenisek, A.: The existence and uniqueness theorem in Biot's consolidation theory. Aplik. Matem. **29**, 194–210 (1984)